

Temperature sensitivity improvement in Bragg grating optical fiber coated by magnetron sputtering technique

Odai Falah Ameen ^{1*}

¹Physics department, College of Education for Pure Sciences, University of Mosul, Mosul, Iraq, 41002

ARTICLE INFO

Received: 07/11/2024
Accepted: 31/12/2024
Available online: 14/11/2025
December Issue
[10.37652/juaps.2024.155044.1334](https://doi.org/10.37652/juaps.2024.155044.1334)

 CITE @ JUAPS

Corresponding author

Odai Falah Ameen
odai.ameen@uomosul.edu.iq

ABSTRACT

In this work, our aim was to design and test a silver-coated fiber Bragg grating (FBG) sensor for temperature sensing applications. An FBG of 125 μm diameter was coated with silver by magnetron sputtering technique. Three coating thicknesses of 10, 20, and 30 nm were prepared and examined. Scanning electron microscopy (SEM) images confirmed the improvement in the roughness of fiber peel when the coating level is increased. The samples were analyzed at moderate ambient temperatures of 20, 60, and 100 $^{\circ}\text{C}$ to evaluate the temperature sensitivity in this range. The results indicated that the Bragg wavelength shift increased with silver coating thickness, and the highest sensitivity ($\Delta\lambda_B/T$) was 0.076 nm/ $^{\circ}\text{C}$ for the 30 nm silver-coated fiber. Hence, the temperature sensitivity improves as the silver coating thickness increases.

Keywords: Bragg wavelength shift, Fiber Bragg grating, Metal coating, Temperature sensor

1 INTRODUCTION

Temperature inspection is an important measurement in several thermodynamic, hydrodynamic, and even optoelectronic regimes to ensure the instant value of temperature in these regimes. This is vital to ensure that the specific part of these regimes is working safely, and their temperature are under control. Therefore, a highly sensitive temperature sensor is required to improve the temperature inspection. Conventionally, thermocouples, which are a type of electrical sensor, have been widely used as temperature sensors. However, these types of sensors exhibited several drawbacks, including the thermal conductivity of wires. Therefore, optical fibers have been recently used as a temperature sensor unit due to their ability to transmit fast signal transitions via the speed of photons. Recently, the Bragg grating optical fibers have moved into the spotlight of research on designing highly sensitive temperature sensors [1–3]. In this regard, several methods and techniques have been proposed and tested to improve the temperature sensitivity of the Bragg grating optical fibers. Yulong Li et al. [4]

used a chemical method to improve the temperature sensitivity of nickel-plated FBG. The results showed that increasing the thickness from 2.75 μm to 337.5 μm of the FBG coating led to an increase in temperature sensitivity from 12.33 pm/ $^{\circ}\text{C}$ to 25.86 pm/ $^{\circ}\text{C}$, respectively. Yan Feng, et al. [5] studied the role of metal coating for enhancing the temperature sensitivity of FBG. Prior work has explored FBG-based sensing across diverse coatings and conditions. Studies have modeled SPR-based FBGs using FDTD to detect alcohol concentration in water [6] and examined temperature effects on side-polished FBGs coated with TiO_2 , Pd, and Fe films [7]. Silver-coated FBGs have been proposed for anemometry, where airflow velocity is inferred from Bragg-wavelength shifts [8]. Temperature sensing has also been tested on FBGs coated with SrTiO_3 thin films on the cladding [9]. Additional work used a magnetic-spray method with ZnO and SiC to enhance temperature sensitivity over 59–300 $^{\circ}\text{C}$ [10]. Additionally, FBG designs have been demonstrated for operation from room temperature up to 800 $^{\circ}\text{C}$ [11]. Elevated-temperature durability has likewise

been reported for gold-coated FBGs operating above 500 °C for extended periods [12]. Here, we investigate the temperature sensitivity of FBGs as a function of silver-coating thickness.

2 MATERIALS AND METHODS

2.1 Principle of FBG sensor

The FBG region is formed by periodic modification of the refractive index of the fiber core along the fiber axis. Periodical structures are inscribed within the core of the fiber optic [13]. The periodic modification in the index of refraction is produced by exposing the fiber core to a spatially varying pattern of UV light. This disorder in the refractive index is called a grating. The amount of change due to the refractive index (Δn) obtained (irradiation conditions) depends on several factors, including wavelength, intensity, and the total dose of light irradiation. In 1989, Meltz et al. introduced the fiber Bragg grating to filter specific wavelengths and allow others to pass through the spectrum. The reflected wavelength depends on the grating period and the change in the refractive index [14–17].

The transmitted light in the optical fiber contains several wavelengths. When the light is transmitted through the optical fiber and passes through the grating region, a particular wavelength will be reflected through the Bragg grating, and the other wavelengths will be transmitted through the fiber. The reflected wavelength, which is called Bragg wavelength (λ_B), depends on the grating period and the length of grating (L_g), as shown in Figure 1. The Bragg wavelength (λ_B) is given by Eq. (1) [17, 18].

$$|\lambda_B = 2n_{eff}\Lambda \quad (1)$$

where n_{eff} is the index of refractive of the fiber core, Λ is the periodical grating that forms the distance between the two adjacent grating planes. All the reflected light from the grating region will accumulate constructively to form a back reflection peak, which is the center wavelength (λ_B). The Bragg grating structure functions as a mirror that reflects the specified wavelength and transmits all other wavelengths.

The grating inside the core of the fiber is formed by various methods depending on the laser, optical fiber type, and the particularly pronounced photosensitivity of the fiber. Hill et al. reported that the germanosilicate optical fibers have a photosensitivity to light at 488 nm. Othonos and Kalli showed that the germanium-boron codoping

produced one fiber doping with large index modulations (on the order of 10^{-3}) [15, 19].

The sensing function of FBG is derived from externally applied mechanical or thermal perturbations. Two parameters (n_{eff} and Λ) are responsible for the change in the Bragg wavelength center (λ_B). The shift in (λ_B) due to the effect of strain and temperature of the FBG is given by [17]:

$$\Delta\lambda_B = 2 \left(\Lambda \frac{\partial n_{eff}}{\partial L} + n_{eff} \frac{\partial \Lambda}{\partial L} \right) \Delta L + 2 \left(\Lambda \frac{\partial n_{eff}}{\partial T} + n_{eff} \frac{\partial \Lambda}{\partial T} \right) \Delta T \quad (2)$$

where ΔT is the temperature variation, ΔL is the change in length of the grating. The first term signifies the strain effect on the Bragg wavelength, and the second term signifies the temperature effect. In addition, the physical parameters such as displacement, index of refraction, and magnetic field are recognized by modulating either n_{eff} Λ of the FBG sensors.

The temperature sensitivity of (λ_B) can be written as a partial derivative with respect to temperature [17]:

$$\frac{\Delta\lambda_B}{\Delta T} = 2n_{eff} \frac{\partial \Lambda}{\partial T} + 2\Lambda \frac{\partial n_{eff}}{\partial T} \quad (3)$$

Substituting Eq. (1) in (3), we get:

$$\frac{\Delta\lambda_B}{\Delta T} = \frac{1}{\Lambda} \frac{\partial \Lambda}{\partial T} \lambda_B + \frac{1}{n_{eff}} \frac{\partial n_{eff}}{\partial T} \lambda_B \quad (4)$$

or

$$\frac{\Delta\lambda_B}{\lambda_B} = \frac{1}{\Lambda} \frac{\partial \Lambda}{\partial T} \Delta T + \frac{1}{n_{eff}} \frac{\partial n_{eff}}{\partial T} \Delta T \quad (5)$$

where $\alpha = (1/\Lambda)(\partial\Lambda/\partial T)$ is the thermal expansion coefficient of the fiber and its value is $0.5 \times 10^{-6} \text{C}^{-1}$ for silica. $\xi = (1/n_{eff})(\partial n_{eff}/\partial T)$ is thermo-optic coefficient and its value is $8.6 \times 10^{-6} \text{C}^{-1}$ for a germanium doped silica-core fiber. At $\Delta\epsilon = 0$, Equation (5) can be written as [2,17]:

$$\frac{\Delta\lambda_B}{\lambda_B} = (\alpha + \xi)\Delta T \quad (6)$$

2.2 Fiber material and coating method

FBG is a fiber with various refraction indexes in the core of the fiber along the length, from high-index to low-index. The variation in the refractive index enables the FBG to function as a mirror that reflects specific wavelengths and transmits others. The spacing between the high- and low-refractive-index regions in the

FBG controls the reflecting and transmitting wavelengths. Figure 1 shows the structure of the FBG.

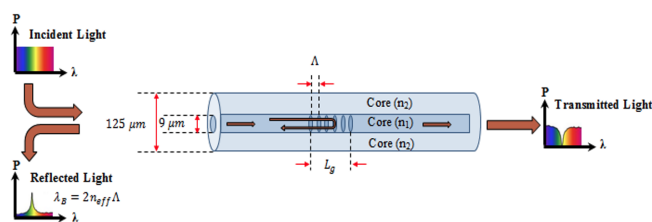


Fig. 1 Structure of fiber Bragg grating (FBG)

Figure 2 shows the system setup used in this work, which consists of a broadband light source (BBLS) to generate wavelengths in the range of 1200-1600 nm. The fiber Bragg grating sensors used in this study are a type of uniform grating made of SMF-28 fiber, with a core diameter of 9 μm and a clad diameter of 125 μm, characterized by a resonance Bragg wavelength λ_B of 1546.025 nm and a grating length L_g of 10 mm. The connectors used in this experiment setup were FC/APC for connecting the FBG sensor and single-mode fibers to the BBLS and OSA. The range of wavelengths of the OSA is 600-1700 nm, with a maximum resolution of 0.02 nm and a fast-scanning rate of 0.2 sec (100 nm span). To test the temperature's influence on the FBG in terms of shifting the center wavelength, the silver-coated FBG sensor was placed in a variable-temperature oven. Silver coating of FBG sensors is a widely used process. Coated FBGs with other metals have been used by others to increase the sensitivity of FBGs and utilize them as temperature sensors.

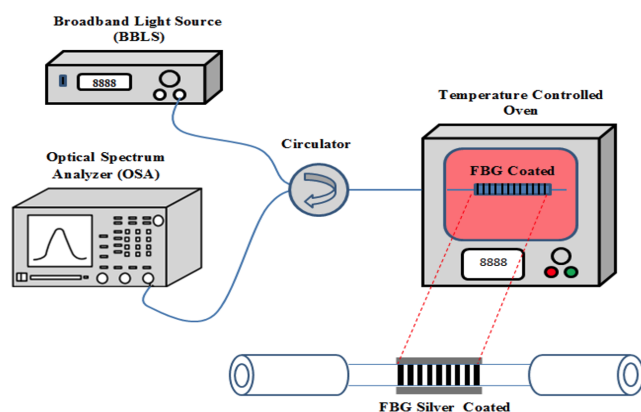


Fig. 2 Experimental setup

2.3 Process of sensor fabrication

A fiber of 1m was used in this study. The fiber sensor was set up as follows: first, the clad of the fiber was removed using the stripper tool T06S13 for a 10 mm length to avoid any possible damage to the fiber core. Second, the fiber was cleaned using methanol and distilled water to remove any possible contamination to obtain a smooth and homogeneous surface. Third, the silver layers were deposited on the sensor region with average thicknesses of 10, 20, and 30 nm at deposition times of 4, 8, and 12 mins, respectively. The deposition process was achieved based on the sputtering coating technique under pressure 1×10^{-2} mbar, current 60 mA, and density 10.50 g/m^3 .

3 RESULTS AND DISCUSSION

3.1 Scanning electron microscopy images

Figure 3 shows the scanning electron microscopy (SEM) images of silver-coated FBG with three different thicknesses, 10, 20, and 30 nm, as shown in a, b, and c, respectively. The results indicated that the shell of the fiber becomes smoother with increased coating thickness.

3.2 Temperature sensitivity results

The three prepared FBG samples were tested at three different temperatures to investigate the effect of the metal coating process on the samples' performance in terms of temperature sensitivity, as measured by the Bragg wavelength shift ($\Delta\lambda_B$). In this sense, we first send a reference spectrum signal (incident spectrum) from BBLS emitted at around 1547 nm (which is the wavelength that causes minimum losses in the optical communication signal). Then the output signal (reflected spectrum) was recorded from the FBG at each temperature. Figure 4 represents the reference spectrum signal for a 10 nm silver-coated FBG and the reflected spectra at 20, 60, and 100 °C. Similarly, Figure 5 presents the reference spectrum signal and the reflected signals for a 20 nm silver-coated FBG, along with the output spectra at 20, 60, and 100 °C. Likewise, Figure 6 represents the reference spectrum for a 30 nm silver-coated FBG and the reflected spectra at 20, 60, and 100 °C. It can be concluded that for all samples, as the temperature increases, the redshift in the reflected spectra and Bragg wavelengths also increases, which could be due to the discontinuity and non-homogeneity of the silver thin film's density, leading to a change in the refractive index of the fiber. However, when the

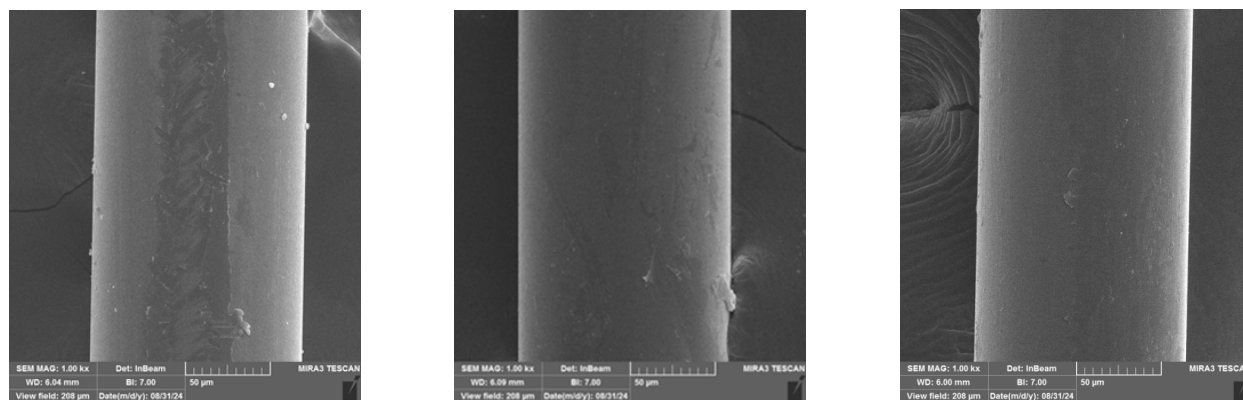


Fig. 3 SEM images for FBG coated with silver at 10 nm (a), 20 nm (b) and 30 nm (c)

coating thickness is increased, the Bragg wavelength shift becomes more obvious. For example, for a 10 nm coated FBG at 20 °C, the shifting in the Bragg wavelength ($\Delta\lambda_B$) was found to be 0.99 nm regarding the reference spectrum, and for a 20 nm coated sample, it was found to be around 1.77 nm, whereas for a 30 nm coated FBG, it was increased to 2.42 nm. This behavior was exhibited for the rest of the tested temperatures (60 and 100 °C) and became more obvious when the temperature increased. These results indicate that the temperature sensitivity of the FBG increases with increasing coating thickness.

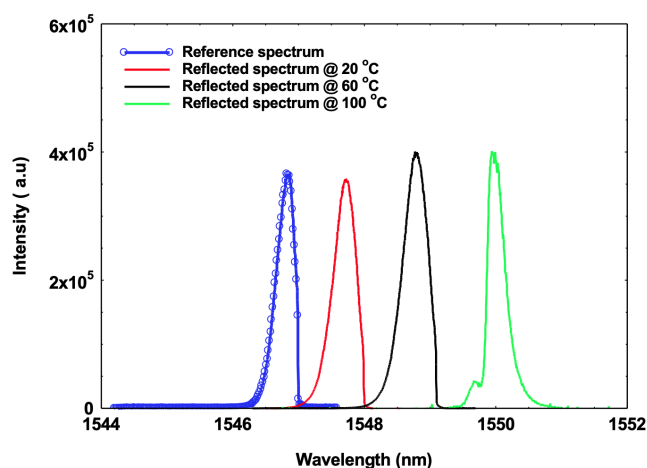


Fig. 4 The incident spectrum and the reflected spectra for 10 nm coated FBG at different temperatures 20, 60, and 100 °C

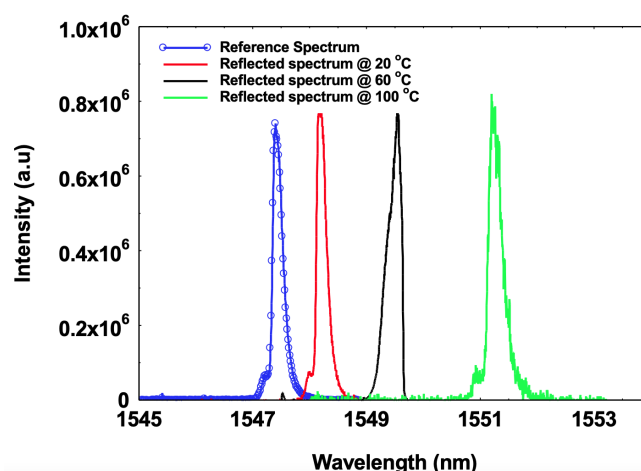


Fig. 5 The incident spectrum and the reflected spectra for 20 nm coated FBG at different temperatures 20, 60, and 100°C

The Bragg wavelengths for the three tested samples were calculated from Figures 4, 5, and 6 and are all listed in Table 1. Additionally, the shifting of the Bragg wavelengths ($\Delta\lambda_B$) at different temperatures for 10, 20, and 30 nm fibers are presented in Table 2.

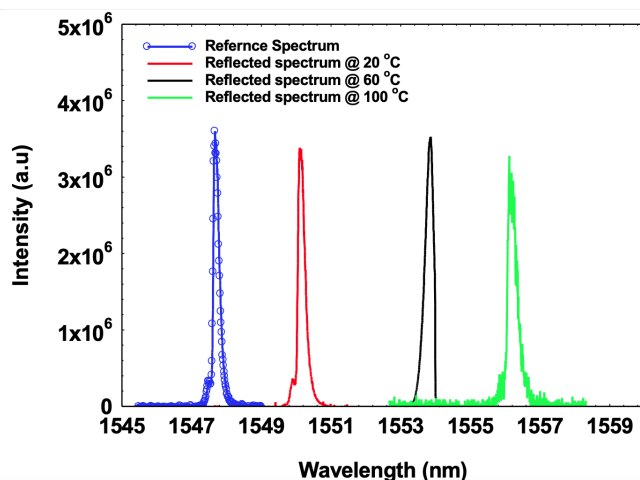


Fig. 6 The incident spectrum and the reflected spectra for 30 nm coated FBG at different temperatures 20, 60, and 100°C

Table 1 The Bragg wavelengths for the three tested samples

Coated FBG (nm)	λ reference (μm)	$\lambda(\mu\text{m})$ at 20 ($^{\circ}\text{C}$)	$\lambda(\mu\text{m})$ at 60 ($^{\circ}\text{C}$)	$\lambda(\mu\text{m})$ at 100 ($^{\circ}\text{C}$)
10	1546.8	1547.79	1548.9	1550.1
20	1546.4	1548.17	1549.56	1551.25
30	1547.7	1550.12	1553.6	1556.2

Table 2 The shifting of the wavelength ($\Delta\lambda$) at different temperatures for 10, 20, and 30 nm fibers

Coated FBG(nm)	$\Delta\lambda B(\mu\text{m})$ at 20 ($^{\circ}\text{C}$)	$\Delta\lambda B(\mu\text{m})$ at 60 ($^{\circ}\text{C}$)	$\Delta\lambda B(\mu\text{m})$ at 100 ($^{\circ}\text{C}$)
10	0.99	2.1	3.3
20	1.77	3.16	4.85
30	2.42	5.9	8.5

For precise analysis of the temperature sensitivity of the FBG samples, the plot of the values of the Bragg wavelength shifting in the reflected spectra ($\Delta\lambda_B$) as a function of the temperature for 10, 20, and 30 nm coated samples is shown in Figure 7. The slopes in Figure 7 represent the temperature sensitivity ($\Delta\lambda_B/T$) of the fibers and are found to be 0.029, 0.038, and 0.076 nm/oC for 10, 20, and 30 nm coated fibers, respectively. The temperature sensitivity increases as the silver coating thickness increases, and the best temperature sensor for FBG is achieved at a 30-nm-coated thickness, as presented in Figure 8.

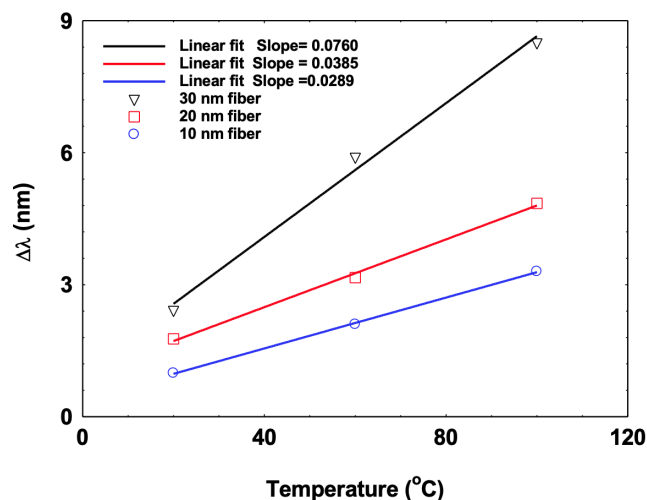


Fig. 7 The values of the shifting in the signal spectra ($\Delta\lambda$) as a function of the temperature for 10, 20, and 30 nm coated samples

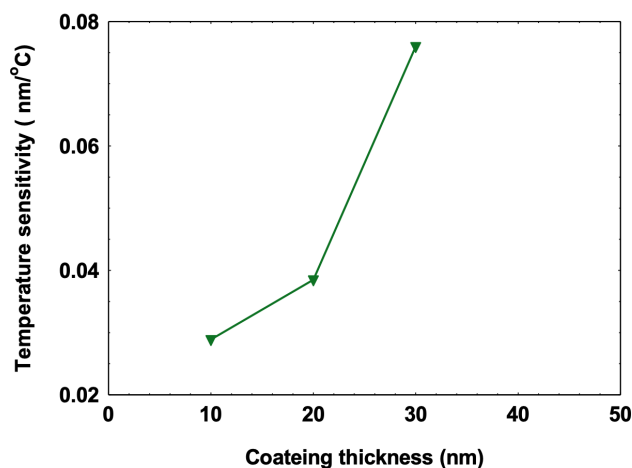


Fig. 8 The temperature sensitivity versus coating thickness of the samples

4 CONCLUSION

Fiber Bragg gratings (FBGs) were metalized with a silver coat using the magnetron sputtering method with three different thicknesses (10, 20, and 30 nm) to examine their ability for temperature sensitivity in temperature sensor applications. SEM images indicated an increase in the roughness of the FBG clad when the thickness of the silver coating increased. It is found that the temperature sensitivity of FBG can be improved by using a silver

coating. Moreover, the Bragg wavelength shifted linearly with temperature, and the temperature sensitivities in terms of the Bragg wavelength ($\Delta\lambda_B/T$) were found to be 0.029, 0.038, and 0.076 nm/°C using plate coatings of 10, 20, and 30 nm, respectively. The results of this study confirm a significant improvement in the FBG for temperature sensitivity when using silver as a metal coating.

ACKNOWLEDGEMENT

We appreciate the obstetrics and gynecology wards and prenatal clinic, Al-Ramadi Teaching Hospital, and Fallujah Teaching Hospital, Anbar, Iraq, for providing abortion swab specimens and the data.

FUNDING SOURCE

No funds received.

DATA AVAILABILITY

N/A

DECLARATIONS

Conflict of interest

The authors declare that they have no known competing financial interests.

Consent to publish

All authors consent to the publication of this work.

Ethical approval

N/A

REFERENCES

- [1] Sheng HJ, Liu WF, Lin KR, Bor SS, Fu MY. High-sensitivity temperature-independent differential pressure sensor using fiber Bragg gratings. *Optics Express*. 2008;16(20):16013. [10.1364/oe.16.016013](https://doi.org/10.1364/oe.16.016013)
- [2] Ameen OF, Younus MH, Aziz MS, Azmi AI, Raja Ibrahim RK, Ghoshal SK. Graphene diaphragm integrated FBG sensors for simultaneous measurement of water level and temperature. *Sensors and Actuators A: Physical*. 2016;252:225–232. [10.1016/j.sna.2016.10.018](https://doi.org/10.1016/j.sna.2016.10.018)
- [3] Feng Y, Toyserkani E, Zhang H, Zhang ZD. Temperature Sensing of Stepped-Metal Coated Optical Fiber Bragg Grating with the Restructured Dual-Peak Resonance. *Applied Sciences*. 2019;9(2):286. [10.3390/app9020286](https://doi.org/10.3390/app9020286)
- [4] Li Y, Hua Z, Yan F, Gang P. Metal coating of fiber Bragg grating and the temperature sensing character after metallization. *Optical Fiber Technology*. 2009;15(4):391–397. [10.1016/j.yofte.2009.05.001](https://doi.org/10.1016/j.yofte.2009.05.001)
- [5] Feng Y, Zhang H, Li YL, Rao CF. Temperature Sensing of Metal-Coated Fiber Bragg Grating. *IEEE/ASME Transactions on Mechatronics*. 2010;15(4):511–519. [10.1109/tmech.2010.2047111](https://doi.org/10.1109/tmech.2010.2047111)
- [6] Arasu PT, Al-Qazwini Y, Onn BI, Noor ASM. Fiber Bragg grating based surface plasmon resonance sensor utilizing FDTD for alcohol detection applications. In: 2012 IEEE 3rd International Conference on Photonics. IEEE; 2012. p. 93–97. [10.1109/icp.2012.6379852](https://doi.org/10.1109/icp.2012.6379852)
- [7] Tien CL, Chen LC, Chiang HY, Liu WF, Shih HF. Temperature sensors based on D-shaped Fiber Bragg Grating coated with different thin films. In: 2012 IEEE Sensors. IEEE; 2012. p. 1–3. [10.1109/ic-sens.2012.6411432](https://doi.org/10.1109/ic-sens.2012.6411432)
- [8] Dong X, Zhou Y, Zhou W, Cheng J, Su Z. Compact Anemometer Using Silver-Coated Fiber Bragg Grating. *IEEE Photonics Journal*. 2012;4(5):1381–1386. [10.1109/jphot.2012.2208946](https://doi.org/10.1109/jphot.2012.2208946)
- [9] Cheng P, Wang L, Pan Y, Yan H, Gao D, Wang J, et al. Fiber Bragg grating temperature sensor of cladding with SrTiO₃ thin film by pulsed laser deposition. *Laser Physics*. 2019;29(2):025107. [10.1088/1555-6611/aaf635](https://doi.org/10.1088/1555-6611/aaf635)
- [10] Mansor NF, Raja Ibrahim RK. Temperature sensitivity of FBG coating with zinc oxide and silicon carbide. *Journal of Physics: Conference Series*. 2021;1892(1):012033. [10.1088/1742-6596/1892/1/012033](https://doi.org/10.1088/1742-6596/1892/1/012033)
- [11] Wang X, Sun X, Hu Y, Zeng L, Liu Q, Duan J. Highly-sensitive fiber Bragg grating temperature sensors with metallic coatings. *Optik*. 2022;262:169337. [10.1016/j.ijleo.2022.169337](https://doi.org/10.1016/j.ijleo.2022.169337)
- [12] Burgess RR, Hulan SA, Mog SJ, Mazingo AN, Thome OG, Bruncz AR, et al. A Gold-Coated FBG Sensor for Heat-Flux Measurement in Harsh Environment. In: 2023 IEEE Photonics Conference (IPC). IEEE; 2023. p. 1–2. [10.1109/ipc57732.2023.10360646](https://doi.org/10.1109/ipc57732.2023.10360646)
- [13] Cuadrado-Laborde C. Current Trends in Short- and Long-period Fiber Gratings. *InTech*; 2013. [10.5772/3320](https://doi.org/10.5772/3320)

- [14] Cusano A, Cutolo A, Albert J. Fiber Bragg Grating Sensors: Recent Advancements, Industrial Applications and Market Exploitation. BENTHAM SCIENCE PUBLISHERS; 2011. [10.2174/97816080508401110101](https://doi.org/10.2174/97816080508401110101)
- [15] Othonos A, Kalli K, Kohnke GE. Fiber Bragg Gratings: Fundamentals and Applications in Telecommunications and Sensing. Physics Today. 2000;53(5):61–62. [10.1063/1.883086](https://doi.org/10.1063/1.883086)
- [16] Meltz G, Morey WW, Glenn WH. Formation of Bragg gratings in optical fibers by a transverse holographic method. Optics Letters. 1989;14(15):823. [10.1364/ol.14.000823](https://doi.org/10.1364/ol.14.000823)
- [17] Rajan G. Optical fiber sensors: advanced techniques and applications. CRC press; 2017
- [18] Ganapathi AS, Maheshwari M, Joshi SC, Chen Z, Asundi A, Tjin SC. Fibre Bragg grating sensors for in-situ measurement of resin pressure in curing composites. In: Quan C, Qian K, Asundi A, Chau FS, editors. International Conference on Experimental Mechanics 2014. vol. 9302. SPIE; 2015. p. 93021T. [10.1117/12.2084783](https://doi.org/10.1117/12.2084783)
- [19] Xie R. Handbook of Advanced Electronic and Photonic Materials and Devices, Vol. 9, Nonlinear Optical Materials. Academic Press: New York.. vol. 9; 2000

How to cite this article

Ameen OF. Temperature sensitivity improvement in Bragg grating optical fiber coated by magnetron sputtering technique. Journal of University of Anbar for Pure Science. 2025; 19(2):102-108. doi:[10.37652/juaps.2024.155044.1334](https://doi.org/10.37652/juaps.2024.155044.1334)